Classical overbarrier model to compute charge exchange and ionization between ions and one-optical-electron atoms

Fabio Sattin*
Consorzio RFX, Corso Stati Uniti 4, 35127 Padova, Italy
(Received 18 January 2000; revised manuscript received 2 June 2000; published 19 September 2000)

In this paper, we study theoretically the process of electron capture between one-optical-electron atoms (e.g., hydrogenlike or alkali atoms) and ions at low-to-medium impact velocities ($v/v_e \approx 1$) working on a modification of an already developed classical overbarrier model [V. Ostrovsky, J. Phys. B **28**, 3901 (1995)], which allows us to give a semianalytical formula for the cross sections. The model is discussed and then applied to a number of test cases, including experimental data as well as data coming from other sophisticated numerical simulations. It is found that the accuracy of the model, with the suggested corrections and applied to quite different situations, is rather high. Furthermore, even ionization can be computed within the same framework.

PACS number(s): 34.70.+e, 34.10.+x

I. INTRODUCTION

The electron capture process in collisions of slow, highly charged ions with neutral atoms and molecules is of great importance not only in basic atomic physics but also in applied fields such as fusion plasmas and astrophysics. The process studied can be written as

$$A^{+q} + B \rightarrow A^{(q-j)+} + B^{j+}. \tag{1}$$

Theoretical models are regularly developed and/or improved to solve Eq. (1) from first principles for a variety of choices of target A and the projectile B, and their predictions are compared with the results of ever more refined experiments.

In principle, one could compute all the quantities of interest by writing the time-dependent Schrödinger equation for the system (1) and programming a computer to solve it. This task can be performed on present-day supercomputers for moderately complicated systems. Notwithstanding this, simple approximate models are still valuable: (i) they allow us to get analytical estimates that are easily adaptable to particular cases; (ii) allow us to get physical insight on the features of the problem by looking at the analytical formulas; (iii) finally, they can be the only tools available when the complexity of the problem overcomes the capabilities of the computers. For this reason, new models are being still developed [1,2].

This paper's author has presented in a recent paper [2] a study attempting to develop a more accurate overbarrier model (OBM) by adding some quantal features. The model so developed was therefore called a semiclassical OBM. Its results showed an improvement with respect to other OBMs.

In this paper, we aim to present an OBM for dealing with one of the simplest processes (1): the one between an ion and a target provided with a single active electron. Unlike the former one [2], this approach is entirely developed within the framework of a classical model, previously studied in [1] (see also [3,4]), but with some important amendments and improvements that, as we shall see, allow to get a quite good accordance with experiments.

II. MODEL

A. Geometry of the scattering

We consider the standard scattering experiment and label **T**, **P**, and **e** respectively the target ion, the projectile, and the electron. The system **T**+**e** is the initial neutral atom. Let **r** be the electron vector relative to **T** and **R** the internuclear vector between **T** and **P**. In the spirit of classical OBMs, all particles are considered as classical objects.

Let us consider the plane $\mathcal{P}$ containing all the three particles and use the projection of cylindrical polar coordinates $(\rho, z, \phi \equiv 0)$ to describe the position of the electron within this plane. We can assign the z axis to the direction along the internuclear axis.

The total energy of the electron is (atomic units will be used unless otherwise stated)

$$E = \frac{p^2}{2} + U = \frac{p^2}{2} - \frac{Z_t}{\sqrt{\rho^2 + z^2}} - \frac{Z_p}{\sqrt{\rho^2 + (R-z)^2}}. \tag{2}$$

Z_p and Z_t are the effective charge of the projectile and of the target seen by the electron, respectively. Notice that we are considering hydrogenlike approximations for both the target and the projectile. We assign an effective charge $Z_t = 1$ to the target and an effective quantum number n to label the binding energy of the electron: $E_n = Z_t^2/2n^2 = 1/2n^2$.

As long as the electron is bound to **T**, we can also approximate E as

$$E(R) = -E_n - \frac{Z_p}{R}. \tag{3}$$

This expression is used throughout all calculations in [1]; however, we notice that it is asymptotically correct as long

*Email address: sattin@igi.pd.cnr.it

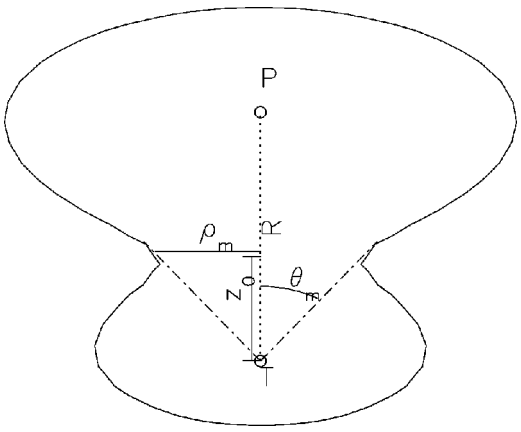

FIG. 1. The enveloping curve shows a section of the equipotential surface $U=E$, i.e., it is the border of the region classically accessible to the electron. R is the internuclear distance. The parameter ρ_m is the radius of the opening that joins the potential wells, θ_m the opening angle from **T**; z_0 is the position of the potential's saddle point.

as as $R\to\infty$. In the limit of small R, instead, $E(R)$ must converge to a finite limit. In the adiabatic approximation $(v/v_e<1)$ it is

$$E(R)\to(Z_p+1)^2E_n \tag{4}$$

(united atom limit). For the moment, we will assume that R is sufficiently large so that Eq. (3) holds, but later we will consider the limit (4), too.

On the plane $\mathcal{P}$ we can draw a section of the equipotential surface

$$U(z,\rho,R)=-E_n-\frac{Z_p}{R}. \tag{5}$$

This represents the limit of the region classically allowed to the electron. When $R\to\infty$, this region is divided into two disconnected circles centered around each of the two nuclei. Initial conditions determine which of the two regions actually the electron lives in. As R diminishes there can be eventually an instant where the two regions become connected. In Fig. 1, we give an example for this.

In the spirit of OBMs, it is the opening of the equipotential curve between **P** and **T** that leads to a leakage of electrons from one nucleus to another, and therefore to charge exchange. We make here the no-return hypothesis: once it has crossed the barrier, the electron does not return to the target. It is well justified if $Z_p\gg1$, much lesser for $Z_p=1$; however, we shall see later how in the case of symmetrical scattering (equal projectile and target) the possibility of the electron return to the target can be accounted for.

It is easy to solve Eq. (5) for R by imposing a vanishing width of the opening $(\rho_m=0)$; furthermore, by imposing also that there be a unique solution for z in the range $0<z<R$:

$$R_m=\frac{(1+\sqrt{Z_p})^2-Z_p}{E_n}. \tag{6}$$

In the region of the opening, the potential U has a saddle structure: along the internuclear axis it has a maximum at

$$z=z_0=R\frac{1}{\sqrt{Z_p}+1}, \tag{7}$$

while this is a minimum along the orthogonal direction.

Charge loss occurs provided the electron is able to cross this potential barrier. Let N_Ω be the fraction of the trajectories that lead to electron loss at the time t. It is clear from the discussion above that it must be function of the solid opening angle Ω, whose projection on the plane is the $\pm\theta_m$ angle. The exact expression for N_Ω will be given below. The quantity we are interested in is $W(t)$: the probability for the electron to be still bound to the target, at time t. Its rate of change is given by

$$dW(t)=-N_\Omega dt\frac{f_T}{T_{em}}W(t). \tag{8}$$

In this expression, dtf_T/T_{em} is the fraction of electrons that cross any surface perpendicular to their motion (and enter the loss region) within time interval dt. T_{em} is the unperturbed period of the electron motion along its orbit, and f_T, a corrective term that accounts for the perturbation: in absence of the projectile it would be $f_T=1$. The unperturbed period can be easily computed by

$$T_{em}=2\int_0^{1/E_n}\frac{dr}{p}=\sqrt{2}\int_0^{1/E_n}\frac{dr}{\sqrt{\frac{1}{r}-E_n}}=2\pi n^3 \tag{9}$$

or, including also $l>0$ orbits:

$$T_{em}=\sqrt{2}\int_{r_{turn}^-}^{r_{turn}^+}\frac{dr}{\sqrt{\frac{1}{r}-E_n-\frac{l(l+1)}{2r^2}}} \tag{10}$$

($r_{turn}^{\pm}$ are the two turning points roots of the square root in the integrand). The parameter f_T must be considered as a free parameter of the model. However, some considerations can be done to justify its presence: first of all, the presence of the projectile deepens the potential energy of the electron, thus the average velocity is likely to be increased and the effective period of revolution reduced: $T_{eff}=T_{em}/f_T<T_{em}$ (this, provided that the average radius of the orbit does not increase sensitively). But another effect contributes to f_T: in Ref. [5], even though addressing a different subject, some studies were performed of the electron trajectory in presence of the projectile field. It was found (see Fig. 5 of that reference, here reproduced in Fig. 2) that the effect of the projectile is not so much evident in varying the electron radial excursion as in varying its angular momentum: in the figure the electron starts with a relatively small angular number (a

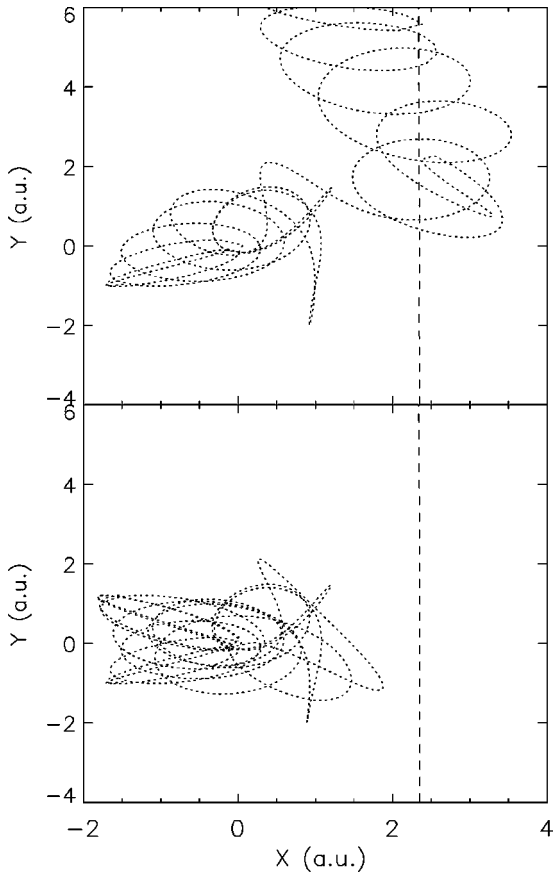

FIG. 2. Two examples of trajectories of the particles **e**, **T**, **P** during the interaction. Upper panel, impact velocity $v=0.10$ a.u., and impact parameter $b=2.345$ a.u. Both **T** and **P** are hydrogen nuclei. The dashed line is the trajectory of the heavy projectile. The electron trajectory is the dotted line. The trajectory of the target nucleus is not shown since it is always close to the origin (0,0). The lower panel shows the same process, but now with $b=2.350$ a.u.

squeezed ellipse) that increases in time, the orbit becoming closer to a circle. We assume an adiabatic collision, so that we can define with reasonable accuracy an instantaneous angular number l function of time. The period T_{em} is too, therefore, a function of time through l. We can therefore assume that the true period at any instant of time be given by Eq. (10): $T_{eff}=T_{em}(l)$. If we start in a condition with $l=0$, we get for l from Fig. 2 an increasing function of time. But, for a given E_n, it can be recovered from Eq. (10) that T_{em} is a *decreasing* function of l so, averaging over the collision time $\overline{T}_{eff}<T_{em}(t=l=0)\rightarrow\overline{f}_T>1$.

A simple integration yields the leakage probability

$$P_l=P(+\infty)=1-W(+\infty)=-\int_{-\infty}^{+\infty}dW(t)$$

$$=1-\exp\left(-\frac{f_T}{T_{em}}\int_{-t_m}^{+t_m}N_\Omega dt\right). \tag{11}$$

In order to actually integrate Eq. (11) we need to know the collision trajectory; an unperturbed straight line with b impact parameter is assumed:

$$R=\sqrt{b^2+(vt)^2}. \tag{12}$$

The extrema $\pm t_m$ in the integral (11) are the maximum values of t at which charge loss can occur.

In the case of symmetrical scattering (equal projectile and target), also P_l must be made symmetrical [1], thus accounting for the possibility of the electron to return to the target:

$$P_l=\frac{1}{2}\left[1-\exp\left(-2\frac{f_T}{T_{em}}\int_{-t_m}^{+t_m}N_\Omega dt\right)\right]. \tag{13}$$

B. Computation of N_Ω

At this point it is necessary to give an explicit expression for N_Ω. In absence of the projectile, the classical electron trajectories, with zero angular momentum, are ellipses squeezed onto the target nucleus. We are thus considering an electron moving essentially in one dimension. Its unperturbed Hamiltonian can be written as

$$\frac{p^2}{2}-\frac{1}{r}=-E_n. \tag{14}$$

The electron has a turning point at

$$r_{turn}=\frac{1}{E_n}. \tag{15}$$

The approaching of the projectile modifies these trajectories. However, in order to make computations feasible, we make the following hypothesis: electron trajectories are considered as essentially unperturbed in the region between the target and the saddle point. The only trajectories that are thus allowed to escape are those whose aphelia are directed toward the opening within the solid angle whose projection on the $\mathcal{P}$ plane is $\pm\theta_m$ (see Fig. 1). Aside from the one on the angle, there is a condition to be fulfilled also on the radial excursion of the electron: it must be able to reach the saddle point. This is equivalent to a condition on the maximum internuclear distance for capture, R_{cap}. Reference [1] considers as captured any electron provided that it has the right direction and that the opening has appeared: thus $R_{cap}=R_m$ [as given by Eq. (6)]. A more restrictive condition is that the electron turning point must be larger than the saddle point. By using Eq. (7) for z_0 and Eq. (15) for the turning radius, we obtain

$$R_{cap}=(\sqrt{Z_p}+1)r_{turn}. \tag{16}$$

We are making here a strong assumption and one that is not fully consistent with the rest of the treatment, since z_0 has been evaluated accounting for the presence of projectile, while r_{turn} holds only in absence of it. However, note that R_{cap} given by Eq. (6) can be written as

$$R_{cap}=(2\sqrt{Z_p}+1)r_{turn}. \tag{17}$$

Both Eqs. (16) and (17) can be interpolated with the single expression

$$R_{cap}=(\alpha\sqrt{Z_p}+1)r_{turn}. \tag{18}$$

Intuitively, using Eq. (17) ($\alpha=2$) should be associated with high values of Z_p: an highly charged ion should strongly attract the electron so that the real behavior of the electron should bear poor resemblance with Eq. (15). On the other hand Eq. (16) ($\alpha=1$) is true in the (unphysical) limit $Z_p \to 0$ and, by extrapolation, could be correct for $Z_p \approx 1$. The question ''What do we mean by $Z_p \gg 1$ and $Z_p \approx 1$?'' is not easy to answer, and probably the answer itself should vary from case to case. For the moment we will keep α as a second free parameter of the model.

The above discussion has been carried on under the hypothesis $l=0$ (apart for the correction due to orbital period): when the angular momentum is different from zero, orbits are ellipses whose minor semiaxis has a finite length. We can still write the Hamiltonian as function of just the radial coordinates (r,p):

$$\frac{p^2}{2}-\frac{1}{r}+\frac{L^2}{2r^2}=-E_n. \tag{19}$$

L is the usual term: $L^2=l(l+1)$. The turning points are now

$$r_{turn}^{\pm}=\frac{1\pm\sqrt{1-2E_nL^2}}{2E_n}. \tag{20}$$

The fraction of trajectories entering the loss cone is much more difficult to estimate in the $l>0$ case. In principle, it can still be determined: it is equal to the fraction of ellipses that have some intersection with the opening. Actual computations can be rather cumbersome. Thus, we use the following approximation, which holds for low angular momenta $l \ll n$ (with n principal quantum number): ellipses are approximated as straight lines (as for the $l=0$ case), and the dependence from l is retained only when evaluating the turning point r_{turn} and the period T_{em}.

The angular integration is now easily done, supposing a uniform distribution for the directions of the electrons:

$$N_\Omega=\frac{1}{2}(1-\cos\theta_m). \tag{21}$$

In order to give an expression for θ_m we notice that $\cos\theta_m = z_0/(\rho_m^2+z_0^2)^{1/2}$, with ρ_m root of

$$E(R)=\left(\rho_m^2+\frac{R^2}{(\sqrt{Z_p}+1)^2}\right)^{-1/2}+Z_p\left(\rho_m^2+\frac{Z_pR^2}{(\sqrt{Z_p}+1)^2}\right)^{-1/2}. \tag{22}$$

It is easy to recognize that, in the right-hand side, the first term is the potential due to the electron-target interaction, and the second is the electron-projectile contribution. Equation (22) cannot be solved analytically for ρ_m except for the particular case $Z_p=1$, for which case;

$$\rho_m^2=\left(\frac{2}{E(R)}\right)^2-\left(\frac{R}{2}\right)^2. \tag{23}$$

The form of $E(R)$ function of R cannot be given analytically, even though can be quite easily computed numerically [6]. In order to deal with expressions amenable to algebraic manipulations, we do therefore the approximation: first of all, divide the space in the two regions $R<R_u, R>R_u$, where R_u is the internuclear distance at which the energy given by Eq. (3) becomes comparable with its united-atom form:

$$E_n+\frac{Z_p}{R_u}=(Z_p+1)^2E_n \to R_u=\frac{Z_p}{(Z_p+1)^2-1}\frac{1}{E_n}. \tag{24}$$

We use then for $E(R)$ the united-atom form for $R<R_u$, and the asymptotic form otherwise:

$$E(R)=\begin{cases} E_n+\dfrac{Z_p}{R}, & R>R_u \\ (Z_p+1)^2E_n, & R<R_u. \end{cases} \tag{25}$$

It is worthwhile explicitly rewriting Eq. (23) for the two cases (remembering that $Z_p=1$):

$$\rho_m^2=\begin{cases} R^2\left(\dfrac{4}{(E_nR+1)^2}-\dfrac{1}{4}\right), & R>R_u \\ \dfrac{1}{4}\left(\dfrac{1}{E_n^2}-R^2\right), & R<R_u \end{cases} \tag{26}$$

and the corresponding expressions for N_Ω are

$$N_\Omega=\frac{1-\cos\theta_m}{2}=\begin{cases} \dfrac{1}{8}(3-E_nR), & R>R_u \\ \dfrac{1}{2}(1-E_nR), & R<R_u. \end{cases} \tag{27}$$

Note that $N_\Omega=1/2$ for $R=0$. This is a check on the correctness of the model, since, for symmetrical scattering at low velocity and small distances we expect the electrons to be equally shared between the two nuclei.

When $Z_p>1$, we have to consider two distinct limits: when $R\to\infty$ we know that eventually $\rho_m\to 0$. It is reasonable therefore to expand Eq. (22) in a series of powers of ρ_m/R and, retaining only terms up to second order:

$$\rho_m^2 \approx \frac{2\sqrt{Z_p}}{(\sqrt{Z_p}+1)^4}R^2[(\sqrt{Z_p}+1)^2-Z_p-E_nR]. \tag{28}$$

Consistently with the limit $R\to\infty$, we have used the large-R expression for $E(R)$.

The limit $R\to 0$ is quite delicate to deal with: a straightforward solution of Eq. (22) would give

$$\rho_m \approx \frac{1}{(Z_p+1)E_n}+O(R), \tag{29}$$

but calculating $\cos\theta_m$, and eventually N_Ω, from this expression gives incorrect results: it is easy to work out the result $N_\Omega=1/2, R\to 0$. This result corresponds to the case in which all and only the electrons going toward **P** are captured. It can be traced back to the united–atom form for $E(R)$: one can notice that the expression thus written is perfectly symmetri-

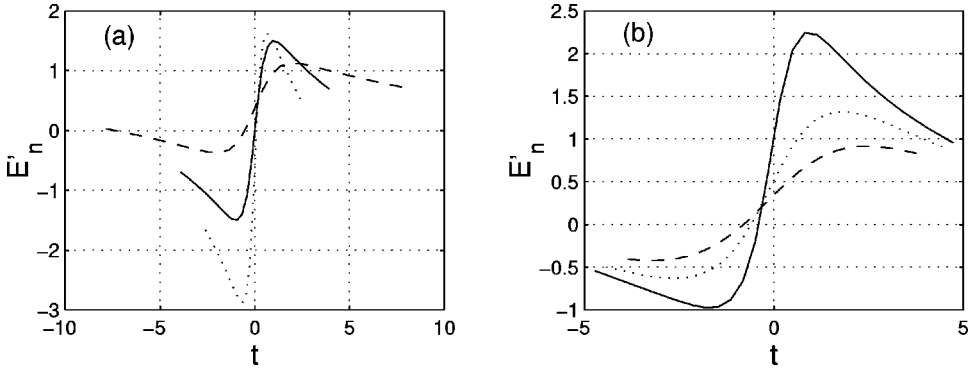

FIG. 3. E' versus time for some choices of the parameters. (a) $E_n=0.5$, $Z_p=1, b/b_m=0.2$, $v=1$ (solid line), $v=1.5$ (dotted line), $v=0.5$ (dashed line); (b) $E_n=0.5$, $Z_p=2$, $v=1$, $b/b_m=0.2$ (solid line), 0.4 (dotted line), 0.6 (dashed line).

cal with respect to the interchange projectile target. Because of this symmetry, electrons are forced to be equally shared between the two nuclei. This is fine when dealing with symmetrical collisions $Z_p=Z_t=1$, and is actually an improvement with respect to [1], where Eq. (28) was used even for small R's and one recovered the value $N_\Omega(R=0)=3/8$. But when $Z_p \gg 1$ the expected result should be $N_\Omega \approx 1$: at small distances the projectile should completely overcome the field of the donor atom so that all electrons should be considered as bound to **P**. This cannot consistently be recovered within our approximations: Eq. (21) does not allow values larger than 1/2 to be obtained. As emphasized in [1], at close encounter the description of electron losses via the trajectory leakage is not natural. However, even though the hypotheses the model is based on break down, we have the possibility of recovering the sought result by extrapolating Eq. (28) to small R, and obtaining

$$\frac{1-\cos\theta_m}{2} \approx \frac{1}{2}\frac{\sqrt{Z_p}}{(\sqrt{Z_p}+1)^2}[(\sqrt{Z_p}+1)^2 - Z_p - E_n R]. \tag{30}$$

It is straightforward to evaluate Eq. (30) in the limit $Z_p \to \infty, R \to 0$, and find the result 1.

We notice that, from the numerical point of view, it is not such a great error using Eq. (28) everywhere: the approximation it is based upon breaks down when R is of the order of R_u or lesser, which is quite a small range with respect to all other lengths involved when $Z_p>1$, while even for the case $Z_p=1$ it is easy to get that the relative error thus introduced on P_l is $\Delta P_l/P_l \approx 1/24$ for small b (and, obviously, it is exactly null for large b). Therefore, Eq. (28) could be used safely in all situations. However, we think that the rigorous although quite lengthy derivation given above was needed since it is not satisfactory working with a model that does not comply with the very basic symmetries of the problem at hand.

C. Corrections for ionization and computation of P_l

Up to now we have implicitly assumed that the rate of *losses* be equal to the rate of *captures*: $dW/dt \equiv dC/dt$. More correctly, one should write $dW/dt = dC/dt + dI/dt$, where dI/dt stands for the rate of ionization. In this section, we derive explicit expression for both dC/dt and dI/dt. It must be noted that already in [1], it was suggested that the model there developed was actually including ionization-via-charge exchange, but to our knowledge, no attempt had been made to separate the two contributions.

Let us thus consider an electron in the saddle point (see Fig. 1). Its energy, in the reference frame of the target, is written as

$$\frac{v_e^2}{2} - \frac{1}{z_0} - \frac{Z_p}{R-z_0} = -E_n - \frac{Z_p}{R}. \tag{31}$$

In the reference frame of the projectile, instead:

$$\frac{(v_e')^2}{2} - \frac{1}{z_0} - \frac{Z_p}{R-z_0} = -E_n' - \frac{1}{R}, \tag{32}$$

where we have labeled with a prime the quantities that refer to the projectile, thus E_n' is the binding energy to **P** and v_e' the relative **e**-**P** velocity. Since $(v_e')^2 = |\mathbf{v_e} - \mathbf{v}|^2 = v_e^2 + v^2 - 2 v_e v \cos\theta$ (θ is the angle between the two velocities), we can substitute it into Eq. (32) which, after rearrangements, becomes

$$E_n' = E_n + \frac{Z_p - 1}{R} - \frac{v^2}{2} + v_e v \cos\theta, \tag{33}$$

with $\cos\theta = vt/R$ (remind that $t<0$ means that **P** is still in the ingoing half of the trajectory). Equation (33), through some simple algebraic manipulations, can be turned into a third-degree polynomial equation for R and therefore for t. One recovers from this equation that, for high enough v—at least for some values of $\cos\theta$—E_n' can be negative, which, of course, is incompatible with capture by the projectile, but can well be associated to ionization. A straightforward assumption is therefore to label as captured just that fraction of electrons for which $E_n' \geqslant 0$. An instructive case is for $Z_p=1, v=1/n$. For this case it is straightforward to see that $E_n'<0$ for $t<0$ and $E_n'>0$ for $t>0$, that is, exactly half of the trajectory contributes to charge exchange. In order to have an idea about the behavior of E', we plot it in Fig. 3 for various combinations of parameters Z_p, b, v. The interpretation of these plots is quite easy: the negative side at $t<0$ appears because of the terms $-v^2/2$ and $v_e v \cos\theta$, both negative. While $t \to -t_m$, E' increases toward zero because $v_e=0$ at $t=-t_m$.

We are finally in the position to define the charge exchange probability from Eq. (11):

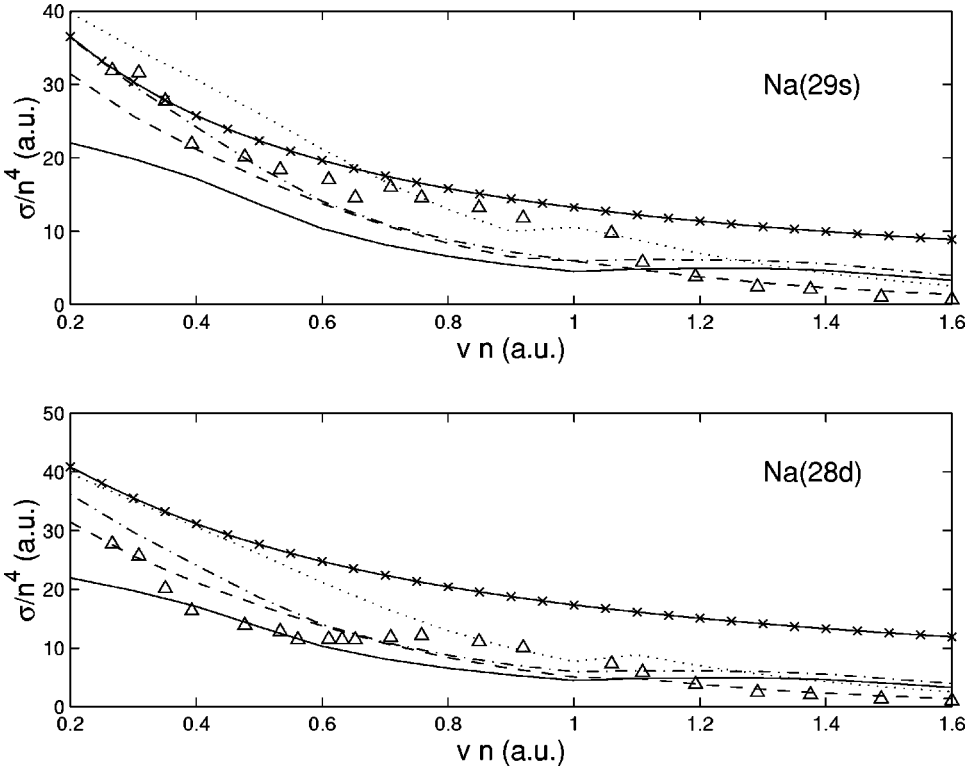

FIG. 4. Cross section for charge exchange for Na^+-Na($29s$) (upper) and Na^+-Na($28d$) (lower) collisions. Symbols, experimental data; solid line, present model with $\alpha=1, f_T=2$; dashed line, $\alpha=2, f_T=1$; dotted line, $\alpha=2, f_T=2$; dotted–dashed line, $\alpha=1, f_T=2$ but without symmetrization of the loss probability. Dotted curve with x's, $\alpha=1, f_T=2$ without allowance for ionization (all losses are attributed to charge exchange). For the definition of α, f_T, see the main text. Note that the experimental results are not absolutely calibrated, the data shown here are calibrated using as reference the CTMC results at $\tilde{v}=1$ and $nl=28d$.

$$P_{CX} = -\int_{t_{CX}^i}^{t_{CX}^f} dW(t)$$
$$= -\exp\left(-\frac{f_T}{T_{em}}\int_{-\infty}^{t_{CX}^f} N_\Omega dt\right) + \exp\left(-\frac{f_T}{T_{em}}\int_{-\infty}^{t_{CX}^i} N_\Omega dt\right)$$
$$= \exp\left(-\frac{f_T}{T_{em}}\int_{-\infty}^{t_{CX}^i} N_\Omega dt\right)\left[1-\exp\left(-\frac{f_T}{T_{em}}\int_{t_{CX}^i}^{t_{CX}^f} N_\Omega dt\right)\right]. \quad (34)$$

The quantity within the exponential is

$$\int_{t_1}^{t_2} N_\Omega dt = F(vt_2/b) - F(vt_1/b),$$

$$F(u) = \frac{\sqrt{Z_p}}{2(\sqrt{Z_p}+1)^2}\left[[(\sqrt{Z_p}+1)^2 - Z_p]\frac{b}{v}u - \left(\frac{E_n b^2}{2v}\right) \times [u\sqrt{1+u^2} + \operatorname{arcsinh}(u)]\right]. \quad (35)$$

The limits of integration $t_{CX}^{i,f}$ are the limit values of the time at which charge exchange can occur: that is $E_n' \geqslant 0$ for $t_{CX}^i < t < t_{CX}^f$, and are roots of the rhs of Eq. (33). A further condition is also that $t \leqslant \sqrt{R_{cap}^2 - b^2}$. A similar expression holds also for ionization, just with the extrema of integration satisfying to the condition $E' < 0$.

The cross sections can be finally obtained after integrating over the impact parameter (this last integration must be done numerically):

$$\sigma = 2\pi \int b P_l(b) db. \quad (36)$$

The integration extends until the maximum b allowed: $b_{max} = R_{cap}$.

III. SOME TEST CASES

A. Na^+-Na($28d,29s$)

As a first test case we consider the inelastic scattering $Na^+ + Na(28d, 29s)$. We investigate this system since (i) it has been studied experimentally in [7]; (ii) it has been used as test case in [1], thus allowing to assess the relative quality of the fits.

The two experimental curves from [7] are very close to each other, reflecting the fact that the two orbits have very similar properties: the energies of the two states differ by a very small amount, and in both cases $E_n L^2 \ll 1$.

In Fig. 4 we plot the normalized cross section $\tilde{\sigma} = \sigma/n^4$ versus the normalized impact velocity $\tilde{v} = vn = v/v_e$ for both collisions $nl = 28d$ and $nl = 29s$. In order to assess the importance of the different parameters, several cases have been considered: $f_T=2, \alpha=1$ (solid line) (we recall that $\alpha=1$ means approximation of unperturbed electron radial motion, while $f_T=2$ means that the period of rotation is halved with respect to the projectile-free case); $f_T=1, \alpha=2$ (dashed line); $f_T=2, \alpha=2$ (dotted line). All these simulations have adopted the symmetrized form for P_l [Eq. (13)]. The effect of leaving the symmetrization out is not strong [the dotted-dashed curve, using Eq. (11) with $f_T=2, \alpha=1$]. In order to assess the importance of ionization we have also computed σ neglecting ionization altogether (dotted curve with x's) : that is,

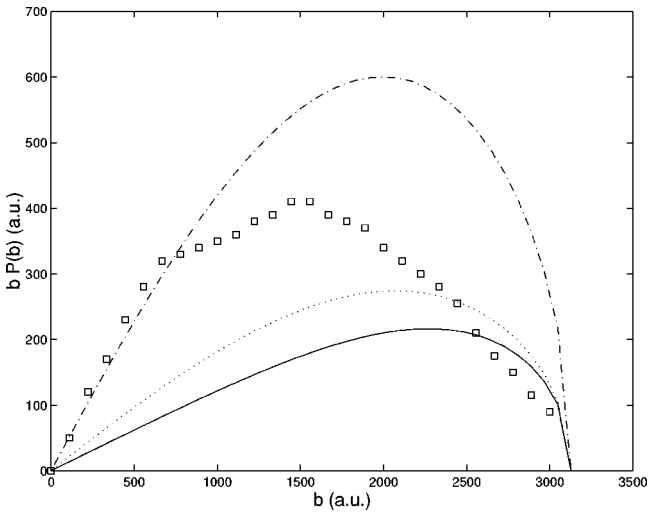

FIG. 5. Differential cross section bP_{CX}, for Na^+-Na($28d$) collision at $\tilde{v}=1$. Squares, CTMC data; solid line, present model with $\alpha=1, f_T=2$; dotted line, the same as previous curve but without symmetrization of P_l; dashed-dotted line, the same as solid curve but adding together charge exchange and ionization.

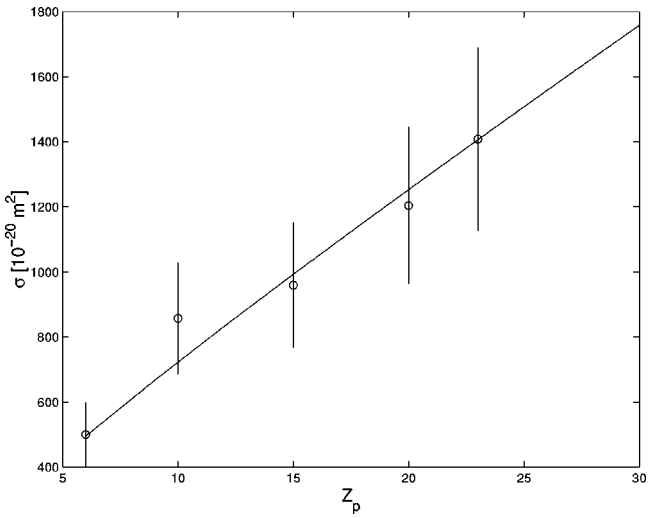

FIG. 6. Cross section for charge exchange in I^{+q}-Cs collisions. Circles, experimental data with 20% error bar; solid line, present model.

all losses were considered as captures. The other parameters were $f_T=2, \alpha=1$. It is apparent how, besides an overall better fit, using Eq. (34) definitely improves the high-velocity ($\tilde{v} \geqslant 1$) range. As for the other curves, differences are quite small and it is impossible from this plot alone to prefer a choice of parameters with respect to the others.

Unlike f_T, α admits a straightforward geometrical representation: the maximum impact parameter at which electron capture can occur is R_{cap} of Eq. (17); therefore we can compute the differential cross section $d\sigma/db = bP_{CX}$, compare it with other independent calculations and check the accuracy of our guess for α. Such a comparison is done in Fig. (5) using as benchmark the CTMC simulations done by Pascale *et al.* [8] for Na^+-Na($28d$) collisions. The choice $\alpha=1$ is perfectly consistent with the maximum impact parameter obtained from CTMC data. This, again, is consistent with the findings of Ref. [5]: at least in these cases, the electron capture process does not appear as a gradual shift of the electron toward the projectile as it is approaching. Instead, the electron appears more like it is following a nearly unperturbed trajectory until it suddenly ''jumps'' (i.e., passes from one nucleus to the other over a relatively short scale of time) to the projectile.

It is worthwhile pointing out here that in [1] the issue of l-changing collisions was extensively discussed, with regard to its importance on suppressing charge exchange at large impact parameters. It was stated that the model there developed could not deal with these transitions and therefore it was expected to give good results only in cases where l transitions were suppressed by the nature of the problem at hand. One can see that we have tackled in this paper the problem of l-changing collisions through f_T and, above all, α parameters. It is the latter parameter that is devoted to the task of suppressing charge exchange at large b's.

Even in this case, we see that explicitly accounting for symmetrization of P_l does not yield great differences (compare solid and dotted curves). What is really important is the inclusion or not of the ionization (dotted-dashed curve). If we assume the CTMC to give the most correct estimate we can conclude that we are overestimating the losses for ionization at small impact parameters. Notice, however, that our approach is entirely based on velocity-matching arguments. The importance of velocity matching is well known for collisions at low velocity with aligned Rydberg atoms [9]. At $v \approx v_e$ and higher, the projectile is likely to transfer an appreciable amount of momentum to the electron. This goes in the direction of reducing the relative **e**–**P** velocity. It should therefore favor charge exchange at the expenses of ionization and alleviate the discrepancy.

B. Iodine-cesium collisions

We apply now our model to the process of electron capture

$$I^{q+} + Cs \rightarrow I^{(q-1)+} + Cs^+ \tag{37}$$

with $q=6-30$. This scattering process has been studied experimentally in [10,11]. It is particularly interesting to study in this context since it could not be tackled satisfactorily by a number of other OBMs, including that of [1] (for a discussion and results, see [2]). The impact energy is chosen equal to $1.5Z_p$ keV: since it corresponds to $\tilde{v} \ll 1$, we expect that ionization does not play any role. The cesium atom is in its ground state with the optical electron in a s state.

In Fig. 6, we plot the experimental points together with our estimates. In this case the fit is excellent using $f_T=2, \alpha=1$. It is important to notice that this agreement is entirely a consequence of our choice for α: to understand this fact, observe that because of the very high charge of the projectile, the exponential term in Eq. (34) is small (F, by direct inspection, is increasing with Z_p) and thus $P_l \approx 1$ over nearly

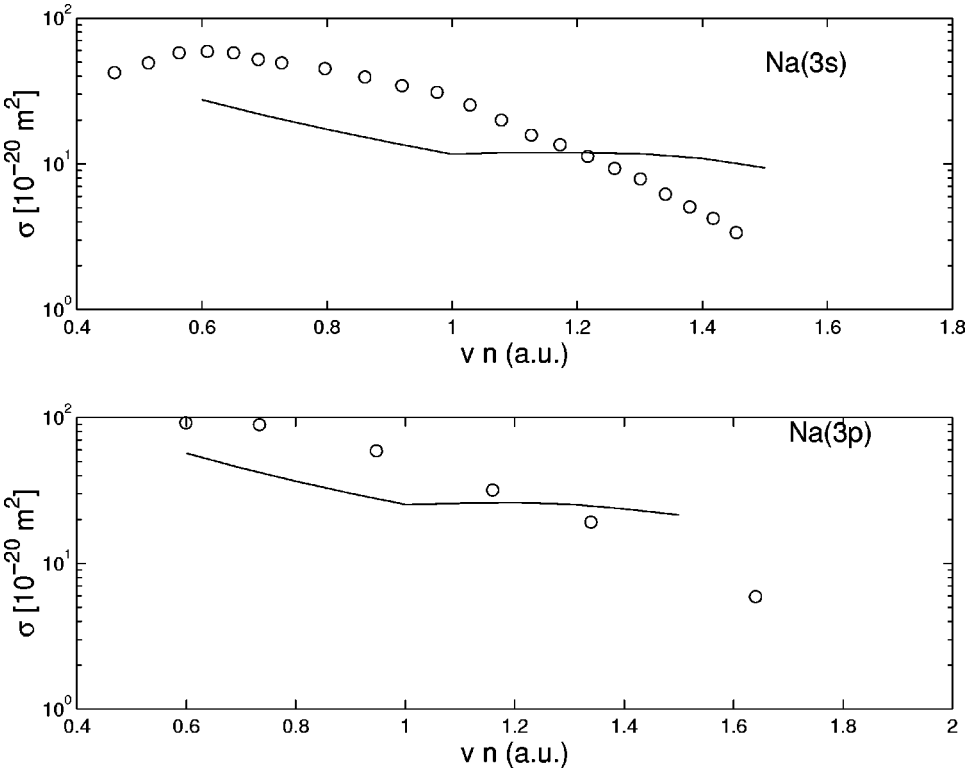

FIG. 7. Cross section for charge exchange in H^+-Na($3s$) (upper) and H^+-Na($3p$) (lower) collisions. Symbols, experimental data; lines, present model.

all the range of bs. The details of the model (in particular of the other free parameter, f_T) which are in F are therefore of no relevance. The only surviving parameter, and that which determines σ, is α. Even though in this case we have no independent estimates of the differential cross section $d\sigma/db$, this suggests that even in this case our choice is correct. Since here we are not dealing with small Z_p, this seems to imply that the parameter α must be a possibly complicated function not only of Z_p but also of E_n, v.

C. H^+–Na($n=3$) collisions

As a further test case we present the results for collisions H^+–Na($3s$,$3p$). They are part of a set of experiments as well as numerical simulations involving also other singly charged ions: He, Ne, and Ar (see [12] and the references therein and in particular [13]; Ref. [14] presents numerical calculations for the same system). In Fig. 7, we plot the results of our model together with those of Ref. [12]. The low-energy wing of the curve is strongly underestimated, while the agreement is somewhat better as v increases, but the slope of σ for relative velocities higher than 1 could not be reproduced.

We do not show results for other ions: they can be found in Fig. 3 of Ref. [12]. What is important to note is that differences of a factor two (and even larger for 3s states) appear between light (H^+,He^+) and heavy (Ne^+,Ar^+) ions, which our model is unable to predict. The suspect is therefore that the structure of the projectile needs to be incorporated into the model. Until now, the only parameter characterizing the projectile has been its charge Z_p. It seems that, as emphasized in [12,13], the energy defect ΔE of the process (the difference of energy between the state bound to the target and that to the projectile) is a crucial parameter: captures to states with $\Delta E \approx 0$ are strongly preferred. Obviously, the value of ΔE depends on the energy levels structure of the recombining ion.

D. H-Be^{4+} collisions

Up to now we have introduced the possibility of ionization just as a means to reduce the probability of charge exchange, but we have not compared the predictions of the model with experimental results. We now address the processes

$$H + Be^{4+} \rightarrow H^+ + Be^{3+} \rightarrow H^+ + e^- + Be^{4+}. \qquad (38)$$

These processes have been studied by Krstic *et al.* [15] using the adiabatic superpromotion model, for $v \leqslant 2$; the molecular approach to the solution of the Schrödinger equation has instead been adopted by Harel *et al.* [16] in the range $v \leqslant 1$ and only for charge exchange.

This system reveals interesting features also with reference to the previous discussion about the correct capture distance R_{cap}: in Fig. 8, we plot results for charge exchange and ionization from the two cited references as well from the present model using for R_{cap} both values $\alpha = 1,2$. It appears again that $\alpha = 1$ is the more appropriate for charge exchange, while neither choice is entirely satisfactory for ionization, even though $\alpha = 1$ seems, here too, slightly to be preferred.

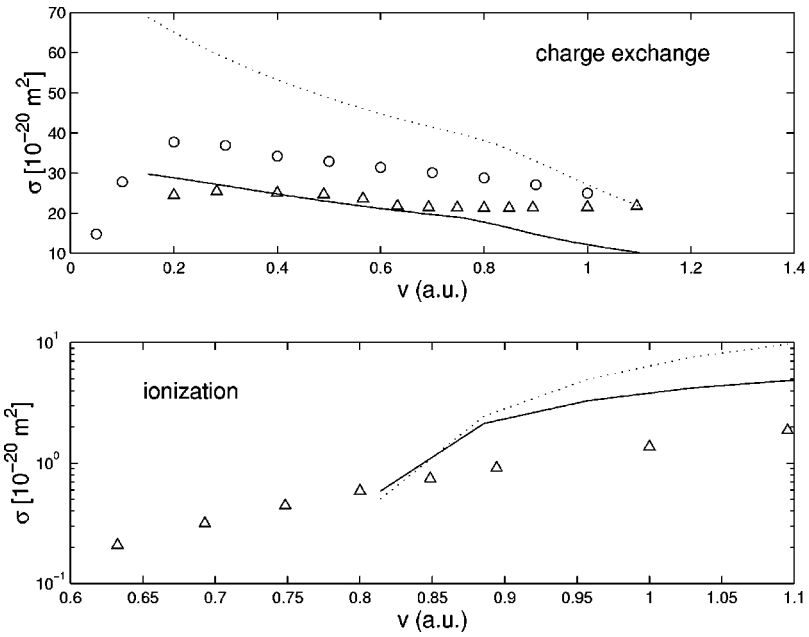

FIG. 8. Cross section versus velocity for Be^{4+}-H(1s) collisions. Upper, charge exchange; lower, ionization. Triangles, data from Ref. [15]; circles, data from Ref. [16]; solid line, present model using $\alpha=1, f_T=2$; dashed line, present model using $\alpha=2, f_T=2$.

The modeling of ionization is not as satisfactory as for charge exchange: in particular, ionization is forced to be zero for low enough velocity, since the right-hand-side of Eq. (33) can no longer become negative. On the other hand, as v increases, ionization increases much more than its experimental value. Notwithstanding this, we do not deem entirely negative the prediction by the model: even though the agreement is scarcely better than a factor of three, we are computing at the same time two processes (ionization and charge exchange) that differ among them by an order of magnitude and which are strictly correlated. It is unavoidable that any small error over the latter carries a large error over the former.

IV. SUMMARY AND CONCLUSIONS

We have developed in this paper a classical OBM for single charge exchange and ionization between ions and atoms. The accuracy of the model has been tested against four cases, with results going from good (Fig. 4), to excellent (Fig. 6), moderate (Fig. 8), and poor (Fig. 7). The model is based upon a previous work [1], and adds to it a number of features, which we go to recall and discuss. The minor improvements involve (i) a more accurate treatment of the small impact parameter region for symmetrical collisions; (ii) the explicit—although still somewhat approximate—treatment of the capture from $l>0$ states.

These points are important from a formal point of view but do not seem to be of any importance in actual computations [This sentence, referring to point (ii), could be contradicted by further computations done for high-angular numbers.]

Some other improvements are instead undoubtedly of the utmost importance. (iii) The finite excursion from the nucleus permitted to the electrons, which in this work has been assumed preferentially to be equal to its projectile-free case. This assumption has been confirmed from some independent computations of the differential cross section, so it seems quite firmly established for small Z_p. It is interesting to remark that some recent experiments seem to indicate the exact capture distance can still be overestimated, even within the present model: in [17] some very accurate experiments of nearly-resonant charge exchange were carried on at low velocities between Rydberg rubidium atoms and low-charged ions ($Z_p=1,\ldots,4$). Both the binding energy to the target E_t (i.e., the quantum number of the optical electron in the Rb atom) and to the projectile E_p (the binding energy to the ion after capture) could be measured and varied with fine tuning. Quasiresonance means that capture was found to be strongly preferred for ratios $k=E_t/E_p\approx 1$. This is, of course, a well-known result. OBMs can predict that capture preferentially populates quantum numbers [1,3]

$$n_p = n_t Z_p \left(\frac{2\sqrt{Z_p}+1}{Z_p+\sqrt{Z_p}} \right)^{1/2}. \tag{39}$$

This result has been numerically confirmed by simulations done using the present model. However, the results of Ref. [17] definitely support lower k (i.e., lower n_p for fixed n_t). The reason, Fisher *et al.* suggest, could be due to an overestimate of the capture distance made by OBMs (these authors give a factor of about 1.6) [18].

(iv) The redefinition of the orbital period of the electron: $T_{eff}=T_{em}/f_T$. This assumption could not be tested as directly as the previous one and the more appropriate value for f_T is still unknown. However, the choice $f_T=2$ done in this work proved to be rather satisfactory.

(v) A correction to the capture probability due finite impact velocity. This has permitted us to introduce the process of ionization within the model. This correction is essential to guarantee a good reliability at high impact energy.

Finally, we recall that the treatment of the projectile—or

better the process of the electron-projectile binding—is an aspect which probably awaits for main improvements. We just observe that it is a shortcoming of all classical methods, that they cannot easily deal with quantized energy levels, so the energy defect is a parameter that is not easily implemented within.

ACKNOWLEDGMENTS

It is a pleasure to thank the staff at National Institute for Fusion Science (Nagoya), and in particular Professor H. Tawara and Dr. K. Hosaka for providing the data of Ref. [10].

[1] V.N. Ostrovsky, J. Phys. B **28**, 3901 (1995).
[2] F. Sattin, J. Phys. B **33**, 861 (2000).
[3] H. Ryufuku, K. Sasaki, and T. Watanabe, Phys. Rev. A **21**, 745 (1980).
[4] A. Niehaus, J. Phys. B **19**, 2925 (1986).
[5] F. Sattin and L. Salasnich, Phys. Rev. E **59**, 1246 (1999).
[6] F. Sattin, Comput. Phys. Commun. **105**, 225 (1997).
[7] S.B. Hansen, L.G. Gray, E. Horsdal-Petersen, and K.B. MacAdam, J. Phys. B **24**, L315 (1991).
[8] J. Pascale, R.E. Olson, and C.O. Reinhold, Phys. Rev. A **42**, 5305 (1990).
[9] L. Fourré and C. Courbin, Z. Phys. D: At., Mol. Clusters **38**, 103 (1996); S. Schippers, Nucl. Instrum. Methods Phys. Res. B **98**, 177 (1995); J.C. Houver *et al.*, Phys. Rev. Lett. **68**, 162 (1992).
[10] K. Hosaka *et al.*, National Institute for Fusion Science Report No. NIFS-PROC-44, 2000 (unpublished).
[11] M. Kimura *et al.*, J. Phys. B **28**, L643 (1995); K. Hosaka *et al.*, Fusion Eng. Des. **34-35**, 781 (1997); A. Hiroyuki *et al.*, Fusion Eng. Des. **34-35**, 785 (1997); K. Hosaka *et al.*, Phys. Scr. **T73**, 273 (1997).
[12] J.W. Thomsen *et al.*, Z. Phys. D: At., Mol. Clusters **37**, 133 (1996).
[13] F. Aumayr, G. Lakits, and H. Winter, Z. Phys. D: At., Mol. Clusters **6**, 145 (1987).
[14] A. Dubois, S.E. Nielsen, and J.P. Hansen, J. Phys. B **26**, 705 (1993).
[15] P.S. Krstic, M. Radmilovic, and R.K. Janev, *Atomic and Plasma-Material Data for Fusion* (IAEA, Vienna, 1992), Vol. 3, p. 113.
[16] C. Harel, H. Jouin, and B. Pons, At. Data Nucl. Data Tables **68**, 279 (1998).
[17] D.S. Fisher *et al.*, Phys. Rev. Lett. **81**, 1817 (1998).
[18] Notice, however, that neither CTMC calculations are able to reproduce the results of Fisher *et al.*, although they miss the experimental value by a smaller amount.